Rapid auxin-induced nitric oxide accumulation and subsequent tyrosine nitration of proteins during adventitious root formation in sunflower hypocotyls

Sunita Yadav,[1] Anisha David,[1] František Baluška[2,*] and Satish C. Bhatla[1,*]

[1]Laboratory of Plant Physiology and Biochemistry; Department of Botany; University of Delhi; Delhi, India; [2]Department of Cell Biology; Institute of Cellular and Molecular Botany; University of Bonn; Bonn, Germany

Using NO specific probe (MNIP-Cu), rapid nitric oxide (NO) accumulation as a response to auxin (IAA) treatment has been observed in the protoplasts from the hypocotyls of sunflower seedlings (*Helianthus annuus* L.). Incubation of protoplasts in presence of NPA (auxin efflux blocker) and PTIO (NO scavenger) leads to significant reduction in NO accumulation, indicating that NO signals represent an early signaling event during auxin-induced response. A surge in NO production has also been demonstrated in whole hypocotyl explants showing adventitious root (AR) development. Evidence of tyrosine nitration of cytosolic proteins as a consequence of NO accumulation has been provided by western blot analysis and immunolocalization in the sections of AR producing hypocotyl segments. Most abundant anti-nitrotyrosine labeling is evident in proteins ranging from 25–80 kDa. Tyrosine nitration of a particular protein (25 kDa) is completely absent in presence of NPA (which suppresses AR formation). Similar lack of tyrosine nitration of this protein is also evident in other conditions which do not allow AR differentiation. Immunofluorescent localization experiments have revealed that non-inductive treatments (such as PTIO) for AR develpoment from hypocotyl segments coincide with symplastic and apoplastic localization of tyrosine nitrated proteins in the xylem elements, in contrast with negligible (and mainly apoplastic) nitration of proteins in the interfascicular cells and phloem elements. Application of NPA does not affect tyrosine nitration of proteins even in the presence of an external source of NO (SNP). Tyrosine nitrated proteins are abundant around the nuclei in the actively dividing cells of the root primordium. Thus, NO-modulated rapid response to IAA treatment through differential distribution of tyrosine nitrated proteins is evident as an inherent aspect of the AR development.

Introduction

Some drawbacks have been reported with regard to the method of detection of NO using diaminofluorescein (DAF) as a fluorescent probe. DAF does not bind NO directly. It reacts with its oxidized form i.e., N_2O_3, under oxygenic conditions and cannot be used to image NO under hypoxic or anoxic conditions.[1-3] Oxidation of NO to N_2O_3 is a third order reaction and is likely to be a rate limiting step in the formation of diaminofluorescein-2 triazole (DAF-2T), thus leading to the very slow formation of N_2O_3 at nanomolar NO levels, consequently affecting the real time detection of NO.[3,4] Furthermore, the formation of DAF-2T depends on the pH of the cytosol. N_2O competes with DAF, leading to a reduction in the formation of DAF-2T at pH above 7.[3] N_2O_3 generated DAF fluorescence also depends on the ionic concentration of the buffer being used. A reduction in fluorescence due to N_2O_3 and DAF interaction has also been observed at higher ionic strength. Finally, ascorbic acid (AA) and dehydroascorbic acid (DHA) are known to combine with DAF to form DAF-2-DHAs, and generate fluorescence similar to DAF-2T. So far, only acridine-TEMPO-DTCS-Fe(II) [complex composed of 2,2,6,6-tetramethyl-piperidine-N-oxyl (TEMPO) labeled with acridine and N-dithiocarboxysarcosine (DTCS)-Fe(II)], CuFl [a Cu(II) complex of a fluorescein modified with an appended metal-chelating ligand (FL)], FNOCT (Fluorescent Nitric Oxide Cheletropic Traps) and MNIP-Cu [a Cu (II) complex of 4-methoxy-2-(1H-naphtho[2,3-d]imidazol-2-yl)phenol (MNIP)] have been reported to bind with NO directly.[5,6] Thus, they are highly specific probes for NO detection. The synthesis of a NO specific probe (MNIP-Cu) has been reported recently.[7]
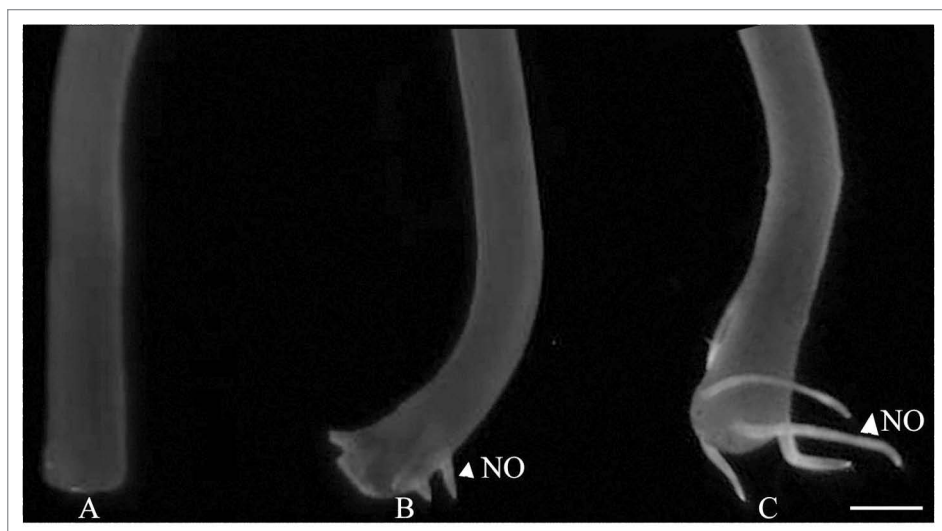
Figure 1. NO distribution in hypocotyl explants at different stages of adventitious rooting. Hypocotyl explants as visualized with MNIP-Cu treatment after 4 (**A**), 5 (**B**) and 7 (**C**) days of incubation in 10 μM of IAA in dark. Scale bar represents 2 mm.

MNIP-Cu can detect NO in vivo without any time lag. It exhibits fluorescence both under anoxic and oxygen rich conditions. This probe is specific to NO, and treatment with PTIO leads to quenching of fluorescence due to MNIP-Cu. It is a relatively non-toxic probe when used at a concentration of 10 μM up to an incubation period of 36 h.[7] Upon binding with NO, MNIP-Cu emits blue fluorescence (ex. 330–385nm; em. 420 nm).

Regulation of protein function by NO-mediated post-translational modifications is a recent area of research in plant biology, and is likely to elucidate the mechanism of NO action in regulating many plant processes. In general, detection of RNS [reactive nitrogen species; S-nitrosothiols (RSNOs), peroxynitrite (ONOO$^-$), N_2O_3 and NO_2] in biological samples is difficult because of the short lifespan of these RNS due to their reactivity with other molecules. Not much is known about RNS in plant cells as compared with animal cells. Several amino acids in proteins can be preferentially nitrated. These include tyrosine, tryptophan, cysteine and methionine. S-nitrosylation is one such modification, which consists of binding of a NO group to a cysteine residue of protein, thereby altering its functions. Tyrosine nitration involves the addition of a nitro group to one of the two equivalents of ortho-carbons of the aromatic ring of tyrosine residues, thus changing tyrosine into a negatively charged hydrophilic nitrotyrosine moiety. Nitration of tyrosine is a selective process. Usually, proteins have approximately 3–4 mol. % of Tyr but only one or two of them become preferentially nitrated, depending on protein structure, nitration mechanism and location of the said protein.[8] Tyrosine nitration is believed to change protein function by gain or no effect and inhibition or stimulation of phosphorylation.

Present work reports about a simple, two step synthesis and application of MNIP-Cu for specific and rapid binding with NO, leading to its detection in plant cells by fluorescence microscopy. Using sunflower hypocotyl segments in adventitious root inducing medium and protoplasts isolated from hypocotyl segments and subsequently subjected to IAA (Indole-3-acetic acid), NPA (1-naphthylthalamic acid) and SNP (Sodium nitroprusside) treatments, present investigations demonstrate the versatile nature of MNIP-Cu in its applications for NO localization. An alternative fluorescent probe for NO detection is, thus, proposed for applications in hypocotyl explants and protoplasts for various physiological investigations. Investigations have further been undertaken to localize differential distribution of tyrosine-nitrated proteins in the hypocotyl segments subjected to AR promoting (IAA and SNP-NO donor) or inhibiting treatments [PTIO (2-(4-phenyl)-4,4,5,5-tetramethylimidazoline-1-oxyl-3-oxide) and (SNP+NPA)]. Experiments have also been conducted to immunolocalize cytosolic proteins by western blot analysis. Both lines of investigations provide new information on the spatiotemporal changes in tyrosine nitration of proteins in response to IAA-NO interaction during AR formation in sunflower hypocotyls.

Results

NO distribution in hypocotyl explants subjected to IAA treatment for induction of adventitious rooting. Hypocotyl explants subjected to 10 μM IAA treatment for 4 d exhibited only internal rooting. In this case, incubation with MNIP-Cu did not lead to any significant fluorescence from the basal cut ends. Five days after incubation, when roots just emerged through the epidermis close to the cut ends of the explants, fluorescence due to NO was evident from the emerging roots (**Fig. 1**). Interestingly, 7 d after incubation in IAA, extensive root extension growth took place and the extreme tips, representing the meristematic zone, showed intense fluorescence due to NO. There is a surge in NO production till the base of the emerging roots.

Auxin treatment brings about rapid NO accumulation in hypocotyl protoplasts. Protoplasts isolated from hypocotyl explants, when co-incubated with IAA (10 μM), showed intense cytosolic blue fluorescence upon treatment with MNIP-Cu. Chloroplasts present in the cytoplasm exhibited red autofluorescence. Thus, blue fluorescence due to MNIP-NO complex was markedly observable and sharply fluorescing entities (mitochondria and oil bodies) were noteworthy in the cytoplasm as compared with the control. Treatment with 10 μM 1-naphthylphthalamic acid (NPA; an auxin efflux blocker) lead to some reduction in fluorescence as compared with control (**Fig. 2**).

Co-incubation of protoplasts with nitric oxide synthase (NOS) inhibitor [N$^\omega$-nitro-L-Arg (L-NNA)] or putative nitrate reductase inhibitor (NaN$_3$) lead to a marked reduction in NO

expression, thereby, indicating that it is primarily synthesized enzymatically. Treatment with 100 μM sodium nitroprusside (SNP; NO donor) did not lead to any marked difference as compared with the control but the fluorescence appeared to be diffuse (**Fig. 2A**). This could be due to the slow and continuous release of NO and its subsequent diffusion into the cytoplasm. In the present work, treatment with the NO scavenger (PTIO) caused a marked reduction of fluorescence in all the treatments (IAA, NPA, SNP), thus confirming that the fluorescence is specific for NO. The data for fluoresecence in all the treatments has been supplemented with a graphical representation (**Fig. 2B**) that signifies the relative fluorescence intensity. The graphical data has been presented as a measure of fluorescence intensity from at least ten protoplasts for a particular treatment.

Tyrosine nitration of proteins in relation with adventitious root formation. Tyrosine nitrated proteins were localized in thin transverse sections obtained from the basal regions of sunflower hypocotyls (derived from 4d old, light-grown seedlings) subjected to treatments which were either inhibitory, partially stimulatory or completely stimulatory for AR formation. Thus, conditions which do not allow the induction of adventitious roots from the interfascicular region, such as treatment with PTIO (a NO scavenger) (**Fig. 3 A–D**) and a treatment with SNP+NPA (**Fig. 3E–H**), clearly showed an abundance of tyrosine-nitrated proteins in the xylem elements of the vascular bundles. The fluorescence was profuse and appeared to be both symplastic and apoplastic in location. In contrast to this, the fluorescence due to tyrosine nitrated proteins was negligible and mainly apoplastic in the interfascicular cells and the phloem elements. There was no significant difference in this pattern of distribution of tyrosine nitrated proteins in the two treatments although SNP acts as an additional source of nitric oxide in one of these treatments. It was further evident that application of the inhibitor of auxin transport i.e., NPA, did not affect tyrosine
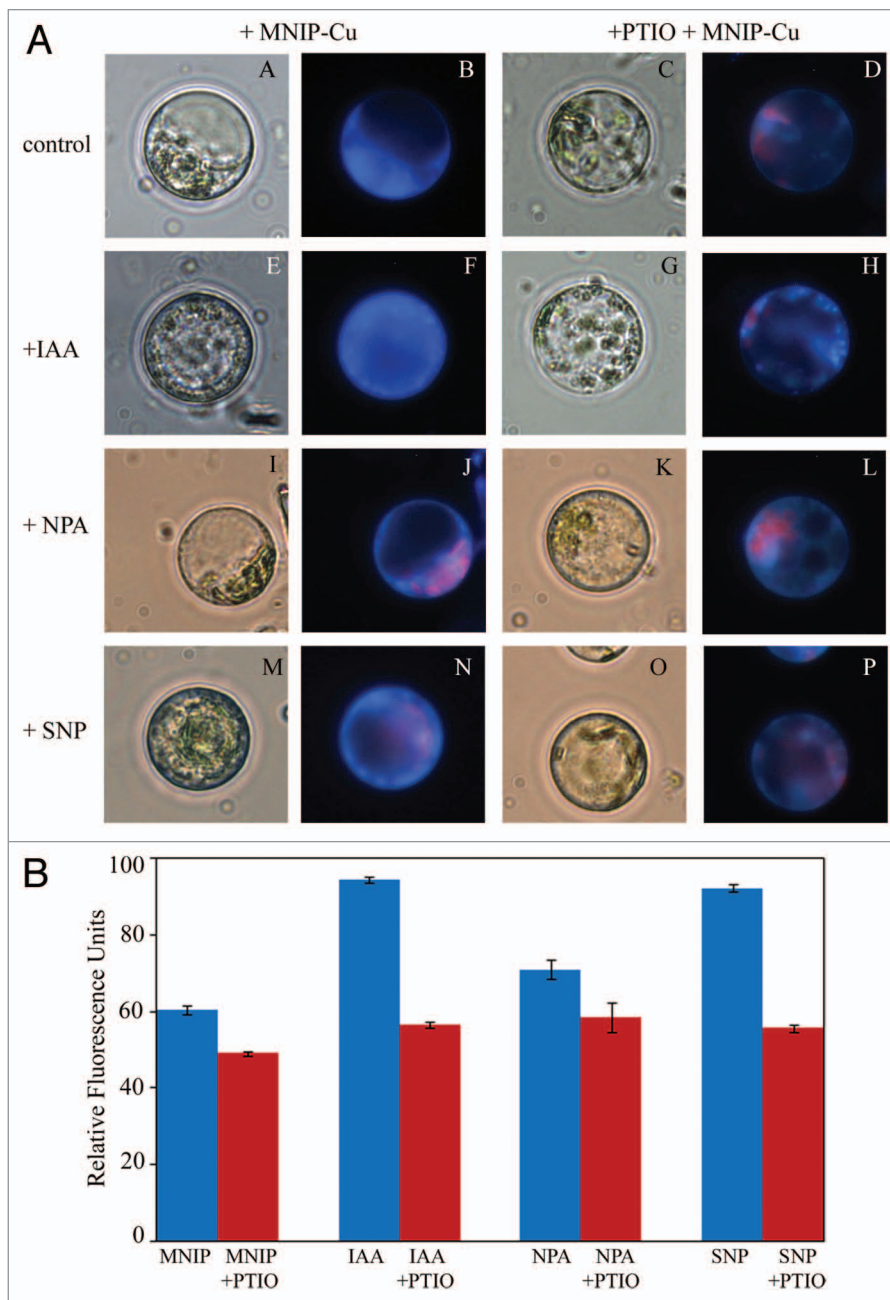

Figure 2. A. Effect of various physiological treatments on NO distribution in protoplasts isolated from the hypocotyls of 4 d old, light grown seedlings. (**A–D**) represent control protoplasts, (**E–H**) are treated with auxin (10 μM IAA). (**I–L**) are treated with auxin influx inhibitor (10 μM NPA) and (**M–P**) are treated with NO donor (100 μM SNP). After incubation in each treatment for 30 min, NO was localized using 25 μM MNIP-Cu and visualized at ex. 365 nm (em. 420 nm) (**B, F, J and N**). Co-incubation with 1 mM PTIO (**D, H, L and P**) confirmed the fluorescence due to NO. All the observations were taken at 630×. B. Relative fluorescence units data from protoplasts subjected to MNIP-Cu treatment for NO localization. Each datum represents mean value and standard errors from ten protoplasts subjected to a particular treatment.

nitration of proteins even in the presence of an external source of nitric oxide i.e., SNP. Application of nitric oxide scavenger i.e., PTIO, did not obstruct root initiation even if the incubation medium contains auxin (**Fig. 3I–L**). Tyrosine nitrated proteins were abundant around the nuclei in the actively dividing cells of

the root primordium. Additionally, the initiation of roots by this treatment (mainly IAA) did not seem to be having any correlation with the presence of tyrosine nitrated proteins evident in the xylem elements of the neighboring vascular bundles where fluorescence due to tyrosine nitrated proteins remained as prominent
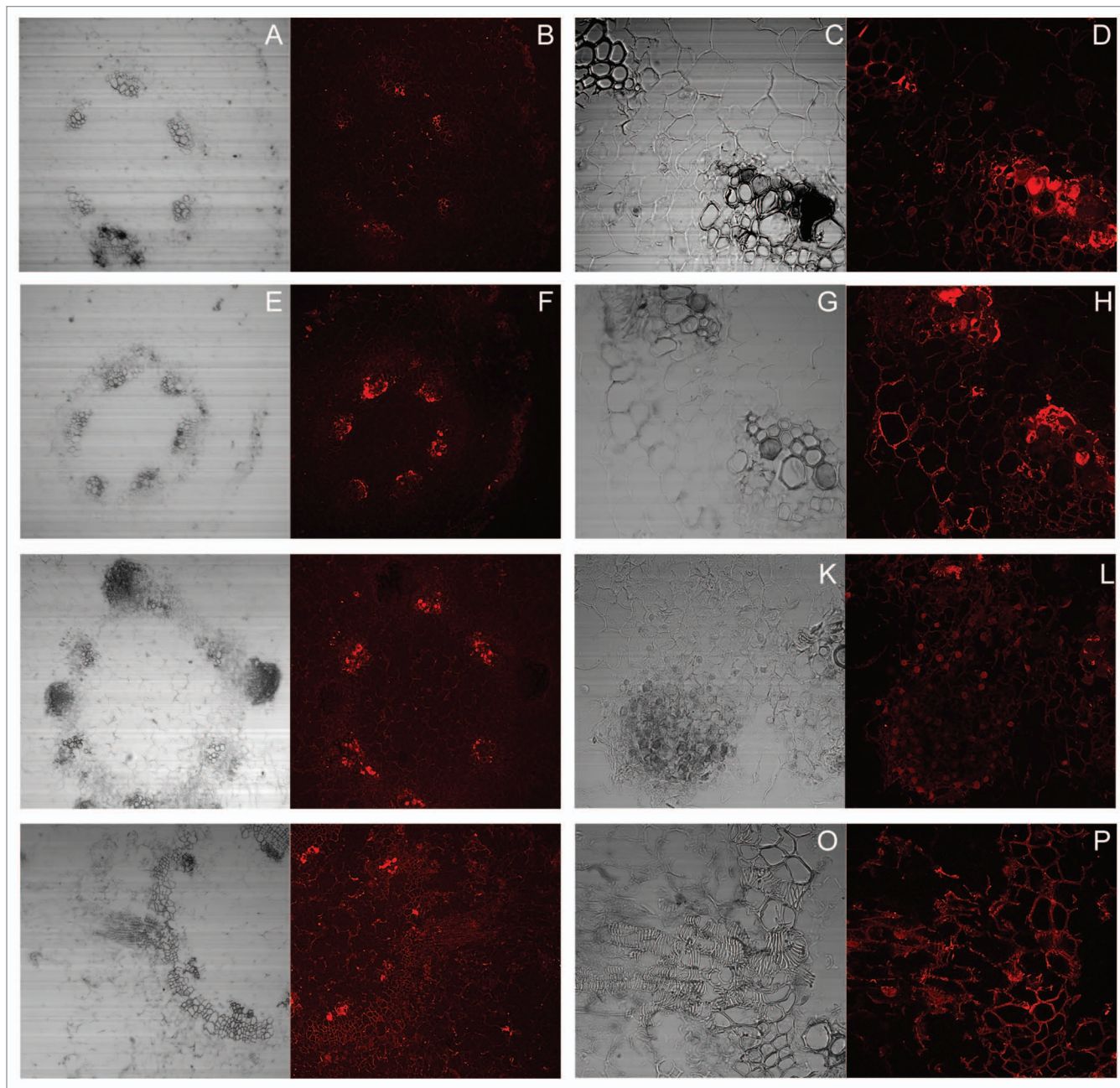
Figure 3. Localization of tyrosine nitrated proteins by CLSM imaging using anti-nitrotyrosine antibody. Visible and fluorescence micrographs of 10 μM thick hypocotyls sections from the basal regions of the explants subjected to treatment of PTIO (1.5 mM) (A-D), SNP (100 μM) + NPA (10 μM) (E-H), SNP (100 μM) + NPA (10 μM) (I-L) and SNP (100 μM) (M-P) in the presence of anti-nitrotyrosine antibody. (**C, D, G, H, K, L, O and P**): Maginified views (400×) of (**A, B, E, F, I, J, M and N**) (100×) respectively, show the differential distribution of tyrosine nitrated proteins in the vascular bundles.

as in conditions where root initials were not being formed. It is during the phase of extension growth of the endogenously arising root initials that the distribution of tyrosine nitrated proteins showed more of a generalized pattern of distribution (**Fig. 3M–P**). As is evident from the images, the fluorescence due to tyrosine nitrated proteins is primarily apoplastic in nature and is evident in practically all the cells.

A comparison with Coomassie stained gels of the separated proteins showed that most abundant anti-nitro tyrosine labeling was evident in proteins ranging from 25–80 kDa (**Fig. 4**). Of

these, noteworthy abundance of tyrosine nitration in treatments triggering adventitious rooting (IAA and SNP) was evident in the protein having a molecular mass close to 25 kDa (**Fig. 4**). In contrast to the abundant tyrosine nitration of this protein in these treatments, tyrosine nitration was completely absent in presence of NPA (a treatment which suppresses AR formation). Similar lack of tyrosine nitration of this protein was also evident in other conditions which did not allow proper AR differentiation (**Fig. 4**). In addition to this, minor differences in the extent of tyrosine nitration were further evident in proteins of high molecular

masses where the AR positive and negative treatments exhibited minor differences.

Discussion

MNIP-Cu is non-toxic at the concentrations applicable for its use (10–50 μM), is cell permeable, directly binds with NO at its intracellular sites rapidly, and the specificity of fluorescence due to MNIP-NO complex is evident from its quenching by PTIO, a well-known NO scavenger. In contrast with DAF, which binds with N_2O_3 (and not NO), MNIP-Cu complexes with NO. MNIP-Cu has, thus, been found to substitute DAF as a probe for localization of NO in hypocotyl explants showing adventitious rooting and protoplasts isolated from sunflower hypocotyl explants. Its synthesis is simple and application straight forward, without any adverse effect on cell viability at the concentration used. Although some reports on NO production accompanying adventitious rooting (as evident using DAF as a probe) are available,[9] so far no attempts have been made to image NO distribution in whole explants, except in *Arabidopsis*.[10] For the first time, spatial distribution of NO has been demonstrated in hypocotyl explants. Adventitious root differentiation coincides with enhanced NO accumulation in the just differentiated and elongating roots from or close to the basal cut ends of hypocotyl explants exhibiting AR development. This auxin-modulated response accompanies rapid NO accumulation, which is also demonstrated from experiments on protoplasts isolated from hypocotyls. Using DAF-2DA as fluorescent probe, enhancement of NO signal has also earlier been observed flow cytometrically, in soybean root protoplasts treated with IAA.[11] Interestingly in this respect, NO and NO-mediated protein modifications are relevant for auxin signaling and polar auxin transport,[12,13] perhaps via their involvement in the control of the cytoskeleton, endocytosis, and vesicle trafficking.[14-16]

The investigations undertaken so far in the limited plant systems as well as animals, have lead to identification of a very limited number of nitrated proteins with different functions.[17,18] In plants, to our knowledge there is no information on the involvement of protein tyrosine nitration during AR development. First account of the identification of proteins which undergo tyrosine nitration in plants under physiological conditions was provided in sunflower.[19] Nitration of abundant proteins, such as those involved in photosynthesis and carbon metabolism, may represent a non-selective scavenging system for reactive nitrogen and oxygen species produced under normal and stress conditions. Earlier work on hypocotyls derived from sunflower seedlings has revealed at least six immunoreactive proteins in the molecular mass range of 15–68 kDa, which undergo tyrosine nitration.[19] Recently, the localization of tyrosine-nitrated proteins in the vascular tissues and cortical cells of hypocotyl
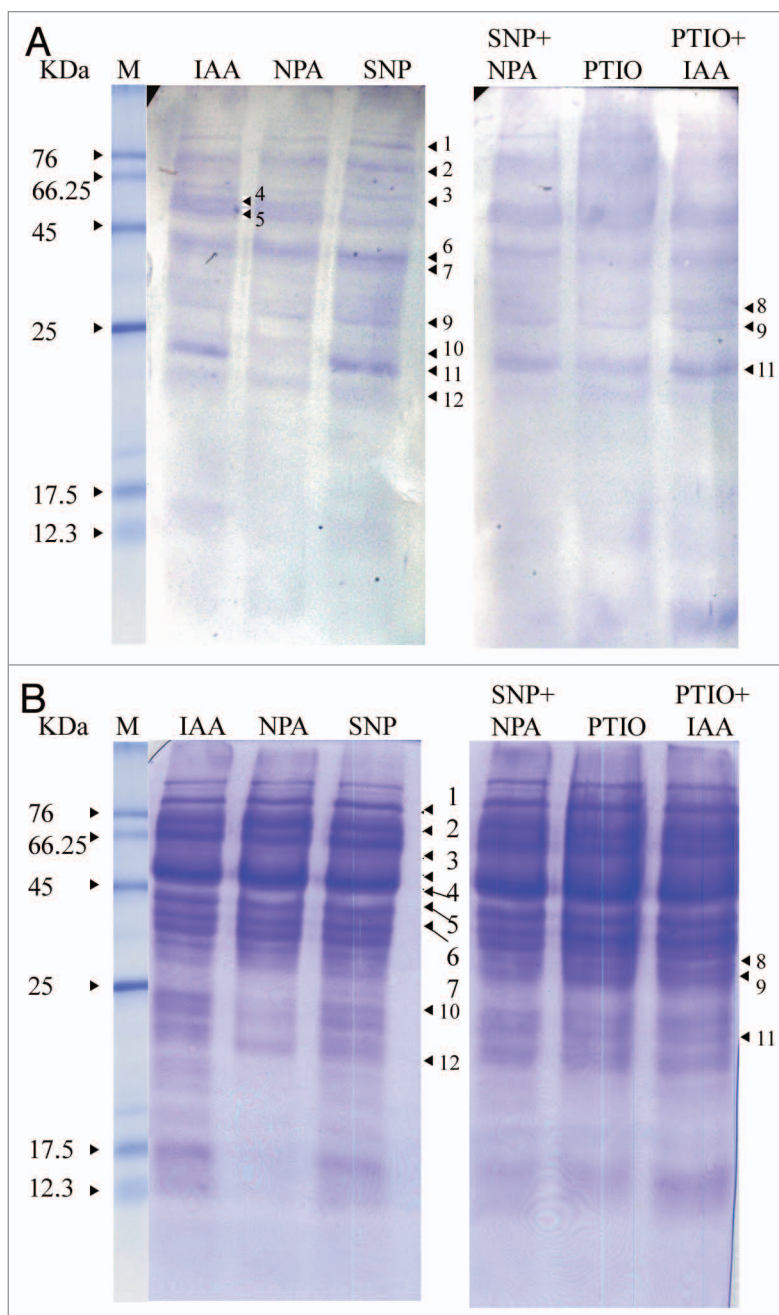

Figure 4. Western blot analyses of anti-nitrotyrosine labeled proteins (**A**) and Coomassie stained gel images (**B**) of hypocotyl segments incubated in IAA (10 μM), NPA (10 μM), SNP (100 μM), SNP+NPA, PTIO (1 mM) and PTIO+IAA for seven days. Other details as in "Materials and Methods." M, marker.

sections was achieved in sunflower.[20] Leaves from salt stressed olive trees have been reported to exhibit tyrosine nitration of proteins of 44–60 kDa.[21] In pea plants grown under several stress conditions (low temperature, high temperature, high light intensity), enhanced tyrosine nitration of proteins has been reported.[22] These observations indicate tyrosine nitration as a marker of nitrosative stress, as has been proposed in animals.[23] Nitration of Rubisco activase, α subunit of ATP synthetase and glutamine synthetase, have recently been identified as putative nitrated proteins

in pathogen-challenged *Arabidopsis*.[24] About 127 proteins have been identified in the proteome analysis from *Arabidopsis thaliana* by immunoprecipitation based on an anti-3-nitro Y antibody. Some of the putative Y-nitrated proteins have been further confirmed by western blot analyses and seven nitrated peptides were identified by MALDI-TOF (Matrix-assisted laser desorption/ionisation-time of flight mass spectrometry).[18] A new level of regulation of primary metabolism is expected to emerge through post-translational nitration of key enzymes and modification of their catalytic properties.

From the present observations it is evident that: 1. Transport of metabolites across the xylem elements coincides with tyrosine nitration of proteins in the concerned cells. 2. The region destined to show root AR initials possesses relatively less tyrosine nitrated protein expression compared with the neighboring vascular bundles. 3. Root initials preferentially show nuclear-localized tyrosine nitrated proteins. 4. The tyrosine nitrated protein expression becomes diffuse and apoplastic during the AR extension phase. Thus, a stage specific distribution and intensification of tyrosine-nitrated proteins is evident in the hypocotyl segments exhibiting AR development. Present observations from the in-gel labeling experiments are in agreement with the differences observed in the spatial localization of tyrosine nitrated proteins in the hypocotyl sections.

To conclude, using a novel NO specific probe (MNIP-Cu) for the first time in plant systems, a rapid NO accumulation has been demonstrated in the hypocotyl protoplasts and AR differentiating zone in response to auxin treatment. The detection of tyrosine-nitrated proteins in sunflower hypocotyl sections obtained through their basal regions subjected to various treatments, which were either, inhibitory, partially stimulatory or completely stimulatory for AR formation, reveals a new level of regulation of AR through post-translational mechanisms. An AR development stage specific distribution and intensification of tyrosine-nitrated proteins is evident in the hypocotyl segments. Most abundant anti-nitro tyrosine labeling is evident in proteins ranging from 25–80 kDa. Noteworthy abundance of tyrosine nitration in treatments triggering adventitious rooting (IAA and SNP) is evident in the proteins having a molecular mass close to 25 kDa. Tyrosine nitration is completely absent in the presence of NPA (a treatment which suppresses AR formation). Present observations from in-gel labeling experiments are in agreement with the differences observed in spatial localization of tyrosine nitrated proteins observed in the hypocotyl sections. These findings present first report on a possible correlation between AR and tyrosine nitration of proteins.

Materials and Methods

Synthesis and characterization of MNIP-Cu: a specific fluorescent probe for detection of nitric oxide. MNIP [4-methoxy-2-(1H-napthol[2,3-*d*]imidazol-2-yl)phenol] was synthesized with minor modifications in accordance with Ouyang et al.[7] A mixture of 2-hydroxy-4-methoxybenzaldehyde (0.316 mmol), 2, 3-diaminonaphthalene [1] (0.316 mmol) and nitrobenzene [2] (2 mL) was refluxed for 2 h. After completion of reaction, the reaction mixture was cooled down to room temperature and diluted

with hexane. The precipitate of MNIP [3] formed was filtered and washed with diethyl ether (**Fig. S1**).

MNIP thus synthesized was characterized by ^{1}H NMR (JEOL Delta Spectrometer, Japan) and IR spectroscopy (2000 FT-IR, Perkin-Elmer). NMR spectra were recorded in *d6*-DMSO, using tetramethylsilane (TMS) as internal standard (refer Supplemental data).

In order to achieve the synthesis of MNIP-Cu, crystals of MNIP were dissolved in dimethyl sulfoxide (DMSO) to obtain a 10 mM stock, which was stored at -20°C. MNIP-Cu was always prepared fresh from MNIP just before use. MNIP stock (10 mM) was diluted to 1 mM with DMSO and 20 μL of 50 mM of aqueous copper sulfate was added to 1 mL of MNIP solution. The mixture was stirred for 5 min at room temperature, resulting in the formation of a stable yellow colored solution of MNIP-Cu.

Characterization of MNIP. MNIP was obtained as light brown solid, 20 mg (22%), mp (296–297°C). IR (KBr) v_{max} (cm^{-1}):3356, 2926, 2373, 1596, 1466, 1399, 1353, 1305, 1261, 1208, 1173, 1136, 1028, 953, 860 cm^{-1}; ^{1}H NMR (400 MHz, DMSO-d_6) δ: 13.48 (brs, 1H, NH), 13.06 (brs, 1H, OH), 8.14 (brs, 1H, ArH), 7.99–8.04 (m, 4H, ArH), 7.37–7.40 (m, 2H, ArH), 6.61–6.64 (m, 2H, ArH), 3.82 (s, 3H, OCH$_3$). The ^{1}H NMR data matched with the one obtained by Ouyang et al.[7]

Detection of NO in hypocotyl explants. Hypocotyl explants at different stages of adventitious rooting from their basal ends in response to 10 μM IAA treatment, were treated with 50 μM MNIP-Cu and visualized for fluorescence due to NO immediately. Visualization of NO fluorescence due to MNIP-NO complex was achieved using UVP EC3 imaging system (ex. 385 nm; em. 420 nm) and imaged using the attached camera.

NO production in hypocotyl-derived protoplasts in response to auxin treatment. Protoplasts were enzymatically isolated from the hypocotyls of 4 d-old, light-grown seedlings.[25] Purified protoplast preparations were treated with 10 μM IAA, 10 μM NPA or 100 μM SNP for 30 min, followed by treatment with 25 μM of MNIP-Cu. Fluorescence due to NO was visualized after exciting at 365 nm (em. 420 nm). For each of the above treatments, incubation with 1 mM PTIO (NO scavenger) for 30 min, followed by co-incubation with MNIP-Cu for 10 min, was also undertaken. All observations were taken on a fluorescence photomicroscope at 630X. MNIP-Cu was found to be tolerable at the concentrations tried (10–50 μM) both in case of whole hypocotyl explants and viable protoplasts. Protoplasts remained viable for more than 3 h when incubated with 25 μM of MNIP-Cu. Whole hypocotyl explants, however, required higher concentration of the probe (50 μM) for optimal fluorescence detection.

Localization of tyrosine-nitrated proteins in wax sections of hypocotyls using antibodies labeled with fluorescent tags. Lower portions (6mm) of hypocotyl explants incubated in 1 mL of various pharmacological agents for 7 d were excised for fixation and subsequent steps.[26] Briefly, the excised tissue was fixed for 60 min in 3.7% formaldehyde prepared in stabilizing buffer (50 mM PIPES, 5 mM MgSO$_4$.7H$_2$O, 5mM EGTA, pH 6.9) for 60 min followed by washing with stabilizing buffer for 30 min and subsequently with phosphate buffer saline [PBS, 0.14 M NaCl, 2.7 mM KCl, 6.5 mM Na$_2$HPO$_4$, 1.5 mM KH$_2$PO$_4$, pH 7.3]

for 15 min. The samples were then dehydrated at 4°C for 30 min each, in an increasing gradation of ethanol (30, 50, 70 and 90%, diluted with PBS). In the final step of dehydration, the samples were transferred into 97% ethanol for 30 min in hot water bath maintained at 37°C. An incubation of 10 min in 0.01% toluidine blue (prepared in 97% ethanol) was performed prior to embedding. Samples were then left in 97% ethanol for 10 min at 37°C. The embedding medium consisted of low melting point Steedman's wax.[27] It was prepared by melting PEG 400 distearate at 65°C and then mixing 1-hexadecanol (9:1, w/w) with continuous stirring for 3–4 h. Wax was then cooled at room temperature and stored. Embedding was initially followed in ethanol/wax (1:1) overnight. Finally, the samples were transferred to 100% wax for 6–7 d. Samples were then placed in the embedding molds and left overnight for polymerization of wax. After embedding, wax ribbons of 10 μm thickness were placed on the slides coated with 0.1% polyethylenimine, and were evenly stretched using a drop of water. The slides were left overnight at room temperature.

Prior to immunolabelling, slides were dewaxed thrice in 97% ethanol, for 10 min each at 4°C. After a 10 min wash in pure ethanol, sections were rehydrated by passing through an ethanol gradation series (90%, 50% ethanol in PBS for 10 min each) and finally PBS (10 min) at 4°C. Before the addition of primary antibody, sections were incubated in a blocking solution (2% BSA in PBS) and then washed in PBS for 5 min and immunolabelling was then performed.[21] Briefly, the sections were incubated with a rabbit polyclonal antibody against 3-nitrotyrosine anti-3NT antibody obtained from Sigma-Aldrich, USA) diluted to 1:300 in PBS containing 0.1% BSA (w/v) for 2 d at 4°C. Subsequently, sections were washed in PBS for 10 min and then incubated with Cy3-labeled anti-rabbit IgG (Amersham) diluted to 1:1000 in PBS containing 0.1% BSA (w/v) for 1 h at room temperature. After labeling, a 10 min rinsing was done in PBS followed by treatment with 0.01% toluidine blue in PBS for 10 min.[28] After washing in PBS for 10 min, the slides were mounted using *p*-phenylenediamine-an anti-fade mounting medium.[29] The sections were visualized using confocal laser scanning microscope (Olympus FluoView, Germany) at excitation 550 nm and emission was monitored at 570 nm.

Western blot analysis for the detection of tyrosine-nitrated proteins. One gram tissue obtained from the basal 6 mm hypocotyl segments incubated for 7 d and (pooled from several explants subjected to specified treatments (IAA, NPA, SNP, SNP+NPA, PTIO, PTIO+IAA), was homogenized in the grinding medium (0.1 M Tris-NaOH, 0.4 M sucrose, 10 mM KCl, 1 mM MgCl$_2$, 1 mM EDTA, 1 mM PMSF pH-7.5 and 0.2% mercaptoethanol) in a proportion of 3 mL g^{-1} FW. The homogenates were filtered through 4 layers of muslin cloth and centrifuged at 10,000 g for 20 min at 4°C (total soluble protein; TSP). The TSP collected as supernatant was acetone-precipitated overnight. Subsequently, the pellet was resolublized in grinding medium, quantified by Bradford method of protein estimation, and constituted in Lamelli buffer. Thirty microgram of each protein sample was loaded for single dimension separation in SDS-PAGE in Miniprotean Tetra Cell (Biorad, USA). The gel was run at 4°C at constant voltage of 75V.

Tyrosine-nitrated proteins were detected through western blotting.[30] Briefly, after running the SDS-PAGE, the gel was sliced out and washed in transfer buffer [20% glycine, 5% tris(hydroxymethyl)aminomethane and 10% methanol] at 4°C for at least 15 min. Meanwhile, PVDF membrane was washed in methanol (100%) for 10 sec, followed by deionized water (5 min) and then in transfer buffer (10–15 min). Filter paper cut to the size of PVDF membrane, was pre-soaked in transfer buffer. The transfer sandwich was prepared by packing together filterpaper (2 pcs), activated PVDF membrane, gel, filterpaper (2 pcs) and placed on the semidry transfer unit platform (ECL semidry Blotter, Amersham Biosciences). A current of 0.8 mA per cm^2 of gel was provided for a period of 4 h at room temperature to achieve complete transfer of proteins. After the completion of transfer, the membrane was removed and stained with Ponceau S (a reversible protein binding stain, prepared by dissolving 0.5% Ponceau S in 1% acetic acid) to monitor proper transfer of proteins. Subsequently the blot was rinsed with MilliQ water to completely remove the stain and then incubated in blocking buffer [2% BSA, 0.01% sodium azide, 0.2% Tween 20 in phosphate buffer saline (PBS, 8 g NaCl, 0.2 g KCl, 1.44 g Na$_2$HPO$_4$, 0.24 g KH$_2$PO$_4$, final volume = 1L) pH 6.8] overnight at 4°C. Blocking prevents non-specific binding of primary and secondary antibodies to membrane. The membrane was then incubated with a rabbit polyclonal antibody against 3-nitrotyrosine (anti-3NT antibody obtained from Sigma-Aldrich) in a dilution of 1:1000 in blocking buffer, for 2 h at room temperature on an orbital shaker. Thereafter, the membrane was washed in wash buffer (0.01% sodium azide, 0.2% tween 20 in PBS pH 6.8) three times for 5 min each and incubated in secondary antibody (anti-rabbit IgG conjugated to alkaline phosphatase antibody) (1:3000 in wash buffer) for 1 h at RT on an orbital shaker. Finally, the membrane was washed in wash buffer three times for 5 min each and developed using freshly prepared BCIP/NBT (1 Sigma Fast tablet dissolved in 10 mL milliQ water) for 10–30 min. BCIP/NBT (5-Bromo-4-chloro-3-indoyl phosphate/Nitro blue tetrazolium) is used as a precipitating substrate for detection of alkaline phosphatase activity. Once the desirable color intensity was obtained, the membrane was placed in MilliQ water. Membrane dried between tissue paper could be stored. Both primary and secondary antibodies were obtained from Sigma-Aldrich (USA).

References

1. Kojima H, Nakatsubo N, Kikuchi K, Kawahara S, Kirino Y, Nagoshi H, et al. Detection and imaging of nitric oxide with novel fluorescent indicators: diaminofluoresceins. Anal Chem 1998; 70:2446-53; PMID:9666719; http://dx.doi.org/10.1021/ac9801723

2. Planchet E, Kaiser WM. Nitric oxide production in plants: facts and fictions. Plant Signal Behav 2006; 1:46-51; PMID:19521475; http://dx.doi.org/10.4161/psb.1.2.2435

3. Vitecek J, Reinohl V, Jones RL. Measuring NO production by plant tissues and suspension cultured cells. Mol Plant 2008; 1:270-84; PMID:19825539; http://dx.doi.org/10.1093/mp/ssm020

4. Mayer B, Hemmens B. Biosynthesis and action of nitric oxide in mammalian cells. Trends Biochem Sci 1997; 22:477-81; PMID:9433128; http://dx.doi.org/10.1016/S0968-0004(97)01147-X.

5. Ye X, Rubakhin SS, Sweedler JV. Detection of nitric oxide in single cells. Analyst 2008; 133:423-33; PMID:18365109; http://dx.doi.org/10.1039/b716174c

6. Vandana S, Sustmann R, Rauen U, Stöhr C. FNOCT as a fluorescent probe for in vivo localization of nitric oxide distribution in tobacco roots. Plant Physiol Biochem 2012; 59:80-9; PMID:22277729; http://dx.doi.org/10.1016/j.plaphy.2012.01.004

7. Ouyang J, Hong H, Shen C, Zhao Y, Ouyang C, Dong L, et al. A novel fluorescent probe for the detection of nitric oxide in vitro and in vivo. Free Radic Biol Med 2008; 45:1426-36; PMID:18804530; http://dx.doi.org/10.1016/j.freeradbiomed.2008.08.016

8. Bartesaghi S, Ferrer-Sueta G, Peluffo G, Valez V, Zhang H, Kalyanaraman B, et al. Protein tyrosine nitration in hydrophilic and hydrophobic environments. Amino Acids 2007; 32:501-15; PMID:17077966; http://dx.doi.org/10.1007/s00726-006-0425-8

9. Huang AX, She XP, Huang C, Song TS. The dynamic distribution of NO and NADPH-diaphorase activity during IBA-induced adventitious root formation. Physiol Plant 2007; 130:240-9; http://dx.doi.org/10.1111/j.1399-3054.2007.00897.x

10. Arita NO, Cohen MF, Tokuda G, Yamasaki H. Fluorometric detection of nitric oxide with diaminofluoresceins (DAFs): Applications and limitations for plant NO research. In: Lamattina L, Polacco JC, eds. Nitric Oxide in Plant Growth, Development and Stress Physiology. Berlin, Heidelberg: Springer-Verlag, 2007:269-80

11. Hu X, Neill SJ, Tang Z, Cai W. Nitric oxide mediates gravitropic bending in soybean roots. Plant Physiol 2005; 137:663-70; PMID:15681661; http://dx.doi.org/10.1104/pp.104.054494

12. Fernández-Marcos M, Sanz L, Lewis DR, Muday GK, Lorenzo O. Nitric oxide causes root apical meristem defects and growth inhibition while reducing PIN-FORMED 1 (PIN1)-dependent acropetal auxin transport. Proc Natl Acad Sci USA 2011; 108:18506-11; PMID:22021439; http://dx.doi.org/10.1073/pnas.1108644108

13. Terrile MC, París R, Calderón-Villalobos LI, Iglesias MJ, Lamattina L, Estelle M, et al. Nitric oxide influences auxin signaling through S-nitrosylation of the Arabidopsis TRANSPORT INHIBITOR RESPONSE 1 auxin receptor. Plant J 2012; 70:492-500; PMID:22171938; http://dx.doi.org/10.1111/j.1365-313X.2011.04885.x

14. Wang Y, Chen T, Zhang C, Hao H, Liu P, Zheng M, et al. Nitric oxide modulates the influx of extracellular Ca^{2+} and actin filament organization during cell wall construction in *Pinus bungeana* pollen tubes. New Phytol 2009; 182:851-62; PMID:19646068; http://dx.doi.org/10.1111/j.1469-8137.2009.02820.x.

15. Kasprowicz A, Szuba A, Volkmann D, Baluška F, Wojtaszek P. Nitric oxide modulates dynamic actin cytoskeleton and vesicle trafficking in a cell type-specific manner in root apices. J Exp Bot 2009; 60:1605-17; PMID:19261922; http://dx.doi.org/10.1093/jxb/erp033

16. Yemets AI, Krasylenko YA, Lytvyn DI, Sheremet YA, Blume YB. Nitric oxide signalling via cytoskeleton in plants. Plant Sci 2011; 181:545-54; PMID:21893251; http://dx.doi.org/10.1016/j.plantsci.2011.04.017

17. Aulak KS, Miyagi M, Yan L, West KA, Massillon D, Crabb JW, et al. Proteomic method identifies proteins nitrated in vivo during inflammatory challenge. Proc Natl Acad Sci USA 2001; 98:12056-61; PMID:11593016; http://dx.doi.org/10.1073/pnas.221269198

18. Lozano-Juste J, Colom-Moreno R, León J. *In vivo* protein tyrosine nitration in *Arabidopsis thaliana.* J Exp Bot 2011; 62:3501-17; PMID:21378116; http://dx.doi.org/10.1093/jxb/err042

19. Chaki M, Valderrama R, Fernández-Ocaña AM, Carreras A, López-Jaramillo J, Luque F, et al. Protein targets of tyrosine nitration in sunflower (*Helianthus annuus* L.) hypocotyls. J Exp Bot 2009; 60:4221-34; PMID:19717529; http://dx.doi.org/10.1093/jxb/erp263

20. Chaki M, Valderrama R, Fernández-Ocaña AM, Carreras A, Gómez-Rodríguez MV, López-Jaramillo J, et al. High temperature triggers the metabolism of S-nitrosothiols in sunflower mediating a process of nitrosative stress which provokes the inhibition of ferredoxin-NADP reductase by tyrosine nitration. Plant Cell Environ 2011; 34:1803-18; PMID:21676000; http://dx.doi.org/10.1111/j.1365-3040.2011.02376.x

21. Valderrama R, Corpas FJ, Carreras A, Fernández-Ocaña A, Chaki M, Luque F, et al. Nitrosative stress in plants. FEBS Lett 2007; 581:453-61; PMID:17240373; http://dx.doi.org/10.1016/j.febslet.2007.01.006

22. Corpas FJ, Chaki M, Fernández-Ocaña A, Valderrama R, Palma JM, Carreras A, et al. Metabolism of reactive nitrogen species in pea plants under abiotic stress conditions. Plant Cell Physiol 2008; 49:1711-22; PMID:18801763; http://dx.doi.org/10.1093/pcp/pcn144

23. Ischiropoulos H. Biological selectivity and functional aspects of protein tyrosine nitration. Biochem Biophys Res Commun 2003; 305:776-83; PMID:12763060; http://dx.doi.org/10.1016/S0006-291X(03)00814-3

24. Cecconi D, Orzetti S, Vandelle E, Rinalducci S, Zolla L, Delledonne M. Protein nitration during defense response in *Arabidopsis thaliana*. Electrophoresis 2009; 30:2460-8; PMID:19598157; http://dx.doi.org/10.1002/elps.200800826

25. Gupta A, Bhatla SC. Spatial and temporal changes in lipase activity sites during oil body mobilization in protoplasts from sunflower seedling cotyledons. Plant Growth Regul 2005; 46:11-7; http://dx.doi.org/10.1007/s10725-005-5231-x

26. Amenós M, Corrales I, Poschenrieder C, Illés P, Baluška F, Barceló J. Different effects of aluminum on the actin cytoskeleton and brefeldin A-sensitive vesicle recycling in root apex cells of two maize varieties differing in root elongation rate and aluminum tolerance. Plant Cell Physiol 2009; 50:528-40; PMID:19176573; http://dx.doi.org/10.1093/pcp/pcp013

27. Baluška F, Parker JS, Barlow PW. Specific patterns of cortical and endoplasmic microtubules associated with cell growth and tissue differentiation in roots of maize (*Zea mays* L.). J Cell Sci 1992; 103:191-200

28. Brown RC, Lemmon BE, Mullinax JB. Immunofluorescent staining of microtubules in plant tissues: improved embedding and sectioning techniques using polyethylene glycol (PEG) and Steedman's wax. Bot Acta 1989; 102:54-61

29. Krenik KD, Kephart GM, Offord KP, Dunnette SL, Gleich GJ. Comparison of antifading agents used in immunofluorescence. J Immunol Methods 1989; 117:91-7; PMID:2464041; http://dx.doi.org/10.1016/0022-1759(89)90122-1

30. Butterfield DA, Sultana R. Identification of 3-nitrotyrosine-modified brain proteins by redox proteomics. Methods Enzymol 2008; 440:295-308; PMID:18423226; http://dx.doi.org/10.1016/S0076-6879(07)00819-1